Hyperfine Interactions in La@C_{82} Studied by W-Band Electron Paramagnetic Resonance and Electron Nuclear Double Resonance†

Norbert Weiden,‡ Tatsuhisa Kato,§ and Klaus-Peter Dinse*,‡

Chemistry Department, Darmstadt University of Technology, Petersenstrasse 20, D-64287 Darmstadt, Germany, and Institute for Molecular Science, Okazaki 444-8585, Japan

Received: July 9, 2003; In Final Form: November 18, 2003

The analysis of dipolar and quadrupolar lanthanum hyperfine data measured with electron paramagnetic resonance (EPR) and electron nuclear double resonance reveals that at low temperatures no significant change occurs at the internal binding site of the endohedral complex. We interpret this result as indicative of freezing of the large-scale motion of the encased ion, which is observed at room temperature. Averaging of hyperfine interactions is fast on the time scale of the EPR experiment, preventing drastic changes of dipolar and quadrupolar hyperfine interaction (hfi), providing that the equilibrium position is unchanged. The detection of hfi in disordered samples was possible by invoking orientation selection in the 94-GHz EPR spectrum. Quadrupolar hfi could be directly measured for the first time in a metallo-endohedral fullerene complex.

Introduction

The problem of localization of the encased metal ion was in the focus of experimental and theoretical studies since macroscopic amounts of metallo-endofullerenes (MEF) became available beginning 1991.[1,2] Direct structure determination via X-ray scattering techniques, as well as indirect spectroscopic studies, have been performed to solve this question.[3] An advantage of less direct methods such as optical spectroscopy and in particular magnetic resonance is given by the fact that these investigations can be performed using highly diluted material. In most cases, a very wide temperature range can also be probed.

The question to be solved can best be stated by describing the potential of the inner fullerene surface seen by the encased atom or ion after inner-molecular charge transfer. Depending on the topology of this potential, either localization or quasifree motion would be possible. Clearly, the binding potential will depend on fullerene topology as well as on the identity of the metal ion, and it could be expected that both extremes of confined particle motion can be realized depending on temperature.

Before pure material in milligram quantities was available, magnetic resonance, which is much less demanding with respect to material quantity, was actually the only experimental tool to address the problem. For this purpose, spectral features, which are influenced by time-dependent terms of the spin Hamiltonian, are analyzed using a model of thermally activated hopping between different binding sites. If the correlation time of this process is fast on the time scale of typical frequency differences in the magnetic resonance spectrum, averaging of spectroscopic properties of different sites occurs. The dynamic process leads to characteristic line broadening, which can be analyzed in terms of different interactions. By a change of the temperature, the correlation time as well as the variance of the time-modulated interactions can be deduced. By this method, it is in principle possible to distinguish between internal hopping of the ion and a tumbling motion of the whole molecule with the ion rigidly attached to its docking position.[4]

Although quite powerful for the fast correlation limit, magnetic resonance investigations based on such a line-shape analysis are limited to a temperature range for which liquid solvents are available. As has been shown, not only a qualitative picture emerged from a spectral fit revealing the concerted action of the anisotropic *g*-matrix, the electron nuclear magnetic dipole, and the nuclear quadrupole interaction but also the principal elements of these second-rank tensors were deduced. At lower temperatures, for which localization is expected, spectral analysis of the rigid-limit spectrum allows to determine these tensor elements directly, thus providing information about the binding site of the localized ion. By a combination of results from a high-temperature dynamic study with rigid limit data, it should be possible to detect the anticipated transition between a temperature-activated large-scale internal motion to rigid attachment from an analysis of the hyperfine tensor elements.

The system La@C_{82}(I) was chosen for this study because of conflicting conclusions published by various groups. X-ray studies by the group of Takata indicated large amplitude motion around a well-defined site (quasilocalization) at room temperature.[5,6] An early theoretical study of Andreoni and Curioni[7] came to the conclusion that the La ion could be localized at two different positions, one of them allowing large amplitude motion. As was shown later,[5] the C_{82} topoisomer investigated in their first study had the wrong cage symmetry (C_2 instead of C_{2v}). In a later study by the same authors,[8] the proper C_{2v} topoisomer was also investigated, apparently exhibiting a unique binding site with strong localization in addition to further local minima, which might be thermally accessible. The hypothesis of hopping between different binding sites was in contradiction to our finding that even at room-temperature molecular tumbling controls the correlation time of the hyperfine interactions (hfi) seen by the ion.[4] The observation of resolved ^{13}C hfi in the EPR spectrum confirmed our model but would still allow large-

† Part of the special issue "Jack H. Freed Festschrift".

* Author to whom correspondence may be addressed. E-mail: dinse@chemie.tu-darmstadt.de.

‡ Darmstadt University of Technology.

§ Institute for Molecular Science.

10.1021/jp035977f CCC: $27.50
Published on Web 03/24/2004

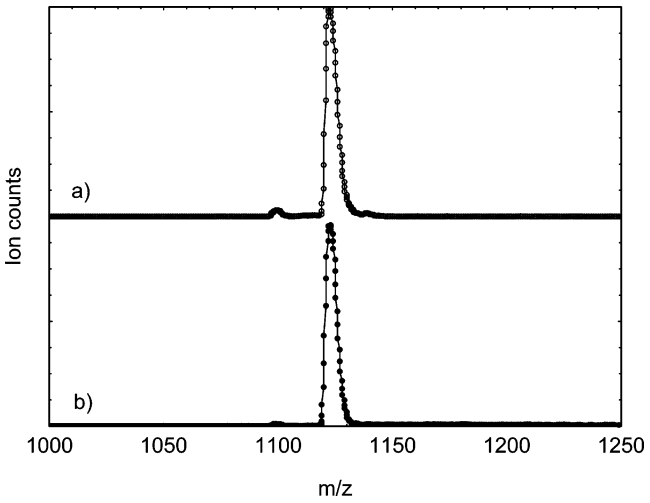

Figure 1. LD-TOF spectra of (a) negative and (b) positive ions of La@C_{82}.

amplitude motion about a defined equilibrium position, which would be in agreement with Takata's room-temperature result.

It was the purpose of this communication to obtain information beyond isotropic dipolar hfi of the encased Lanthanum ion and to test if there is a noticeable change of these values in the range from 300 K down to 4 K. At this low temperature, localization can safely be assumed and any temperature-dependent change of the hfi's could be attributed to incipient delocalization of the ion.

Experimental Section

Soot containing La@C_{82} was prepared by conventional arc vaporization of a rod composed of graphite and La_2O_3 in helium atmosphere. After Soxhlet extraction, a highly purified sample of the major isomer of La@C_{82} (La@C_{82}(I) (C_{2v})) was obtained by employing the high performance liquid chromatographic (HPLC) method described in a previous report.[9] The purity of the sample of more than 99% was confirmed by a laser desorption time-of-flight (LD-TOF) mass spectrometry and electron paramagnetic resonance (EPR) spectroscopy at room temperature in CS_2 solution. Mass purity was confirmed by the observation of a major peak at $m/z = 1123$ in negative- and positive-linear mode mass spectrometry, as shown in Figure 1. The absence of additional peaks in the solution EPR spectrum is proof for the presence of only the major isomer of La@C_{82} (see Figure 2). Diluted solutions of the compound in toluene were degassed on a high vacuum line and subsequently sealed in 4-mm or 0.9-mm o.d. quartz tubes. EPR spectra were taken with a BRUKER Elexsys 680 spectrometer at 9.4 GHz (X-band) and 94 GHz (W-band). W-band-pulsed electron nuclear double resonance (ENDOR) experiments were performed using a home-built ENDOR probe head.[10] ENDOR signals are recorded by monitoring the EPR echo intensity at time delay τ after the last pulse of a 3-pulse ($\pi - T - \pi/2 - \tau - \pi$) sequence. Transitions between nuclear spin levels (ENDOR transitions) are excited by a gated radio frequency (rf) field during time interval T. The ENDOR effect arises because the echo intensity is diminished by rf-induced frequency changes of EPR transitions, thus "refilling" the hole in the inhomogeneous EPR line created by the first inverting microwave pulse. The microwave pulse power of 5 mW provided by the commercial microwave bridge was boosted to a level of 100 mW using a multistage amplifier. The microwave field amplitude at the sample was approximately 0.25 mT, as determined by the $\pi/2$ pulse length of 35 ns.

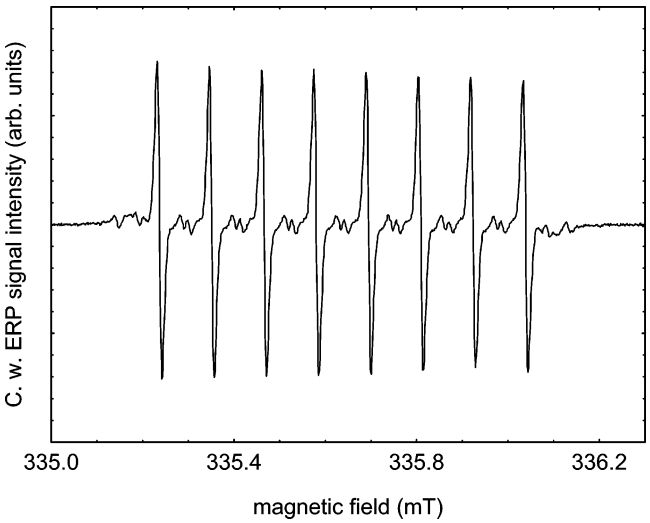

Figure 2. Room-temperature EPR spectrum of the major topoisomer of La@C_{82} in CS_2. Small satellite lines originate form ^{13}C hfi in natural abundance.

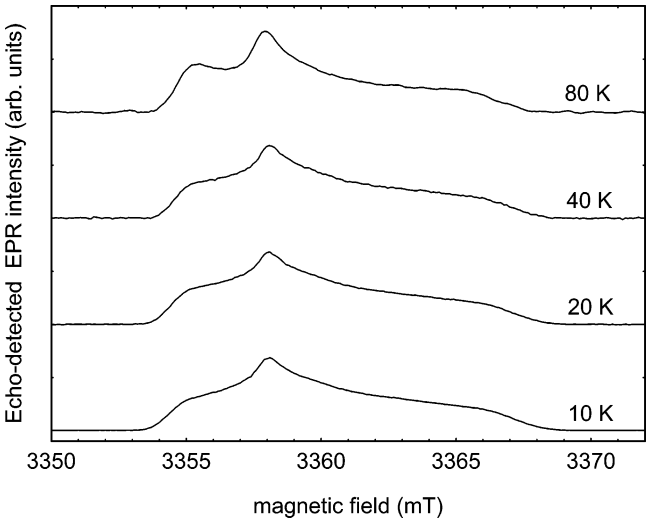

Figure 3. Echo-detected W-band EPR spectra of a frozen solution of La@C_{82}(I) in toluene-d_8 at various temperatures.

Results and Discussion

1. EPR Spectra. As is known from previous studies,[11] no hyperfine information can be extracted from X- and W-band EPR powder spectra of La@C_{82}(I). The reason is that, although g-matrix anisotropy is sufficiently large to lead to a powder pattern in W-band, the Zeeman-related powder pattern is not large enough to dominate hfi-related additional powder broadening even at 3.3 T. In Figure 3, a series of low-temperature EPR spectra is depicted. As can be noted, spectral features of the spectra still changed even below 80 K. Similar observations had already been reported in ref 11. Because spectra in Figure 3 were obtained using a simple 2-pulse echo sequence with fixed pulse delay, apparent intensity variation could result from an orientation-dependent spin-dephasing time T_2. This would be evidence for residual cage mobility and will be subject of further investigation. In addition, the total spectral width is reduced noticeably comparing 80 with 10 K spectra as is shown in Figure 4. This change in g-matrix anisotropy probably indicates structural changes, which occur also in this temperature interval.

The inhomogeneously broadened EPR spectrum extends over approximately 15 mT. Efficient orientation selection by selective excitation of spin packets is still possible considering that the

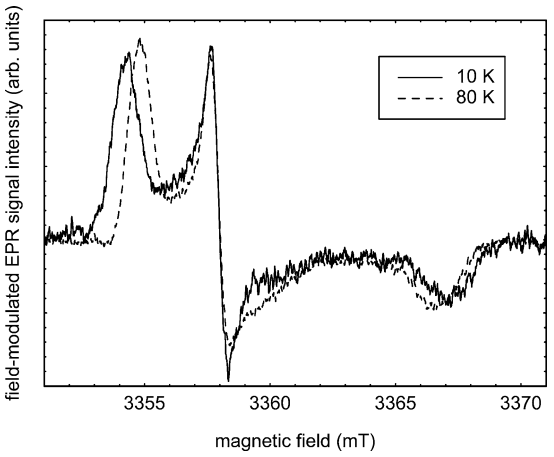

Figure 4. Continuous-wave EPR spectra of La@C_{82}(I) showing the apparent increase of *g*-matrix anisotropy at lower temperatures.

effective spectral width of microwave pulses used for W-band ENDOR is less than 0.5 mT.

2. ENDOR Spectra. Apart from simplifying crowded EPR spectra, ENDOR gives the opportunity to detect electric field gradients (EFG) using the electric quadrupole moment Q of $I > {}^1/_2$ nuclei as local sensor. In ENDOR, a nonvanishing nuclear quadrupole interaction (nqi) leads to two characteristic multiplets of $2I$ lines each, centered at $|\nu_n + A_{zz}(\Theta,\Phi)m_s|$

$$\Delta\nu_{m_I+1,m_I} = |\nu_n + A_{zz}(\Theta,\Phi)m_s + {}^3/_2 Q_{zz}(\Theta,\Phi)(2m_I + 1)| \quad (1)$$

In eq 1, m_I is ranging from $-|I|$ to $|I| - 1$, and only allowed NMR transitions are considered. In both electron spin sublevels, the same characteristic quadrupolar splitting of $3Q_{zz}(\Theta,\Phi)$ between adjacent lines is predicted. The orientational dependence of the interaction terms is denoted by the angles Θ and Φ, relating the eigen axes of the interactions (given as "primed" coordinates) to the laboratory z axis, which in turn is defined by the magnetic field direction. The ENDOR frequencies result when calculating (in first order) eigenvalues of the following spin Hamiltonian under the condition of $\Delta m_s = 0$ and $\Delta m_I = \pm 1$

$$H/h = \nu_e S_z - \nu_n I_z + SAI + IQI \quad (2)$$

Here, in usual notation, the electron and nuclear Larmor frequencies are indicated as ν_e and ν_n, respectively. The dipolar hyperfine coupling tensor (including its isotropic part) is denoted as A, the traceless quadrupole coupling tensor as Q (all values given in frequency units). Its principal value $Q_{z'z'}$ is related to the quadrupole coupling constant eQq/h by $Q_{z'z'} = eqQ/(2I(2I-1)h)$. In eq 2, the orientation dependence of the Zeeman frequencies has been neglected, because ENDOR transitions are not depending on ν_e and the very small dependence of ν_n cannot be resolved in practice.

If efficient orientation selection can be obtained, a "single crystal-like" ENDOR spectrum is predicted, allowing direct determination of the nuclear quadrupole interaction (nqi). Sufficient orientation selection can be obtained if electron Zeeman anisotropy dominates the EPR spectrum and if the principal axes systems of the *g*-matrix and of the nqi tensor are collinear, a situation in the present case granted because of the C_{2v} symmetry of the compound (see below).

As shown in Figure 5, 94-GHz EPR spectra can be reproduced using a nonaxial *g*-matrix. This finding is consistent with the structure model presented by Takata et al., showing that

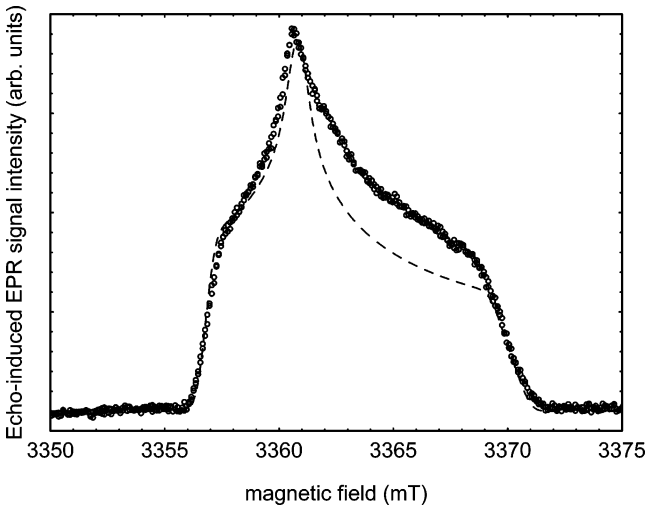

Figure 5. Comparison of experimental and simulated EPR spectra of La@C_{82}(I). The spectrum was measured at 10 K with a microwave frequency of 93.8314 GHz. The magnetic field was calibrated via the ^{2}H ENDOR frequency of distant nuclei. A best fit of canonical positions was obtained using $g_{xx} = 1.99715$, $g_{yy} = 1.99475$, and $g_{zz} = 1.98925$. The shift of the EPR spectrum by 2.5 mT to higher field compared to Figures 1 and 2 results from use of a slightly smaller microwave frequency.

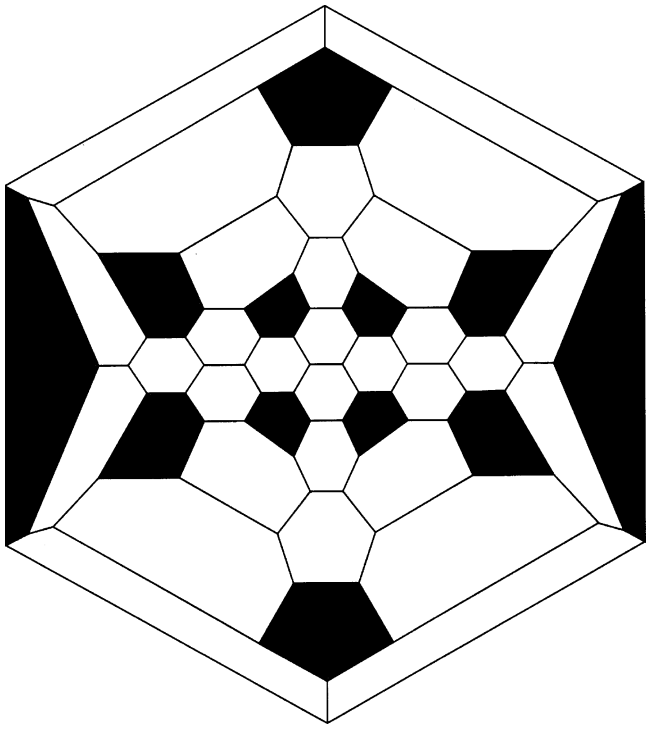

Figure 6. Schlegel diagram of the C_{2v} topoisomer of C_{82}. This cage is found to confine La in case of the major MEF component of this mass. The C_2 axis bisects the 6,6-bond, placed in the center of the diagram. Although no axes assignment can be deduced unambiguously from the spectra, we tentatively assign the smallest principle *g*-matrix value to the C_2 axis direction, thus defining the local z' direction. Calculations predict a displacement of the La ion along the C_2 axis from the center of gravity of the cage toward the six-membered ring.

the La ion is positioned at the C_2 axis of the fullerene cage, thus preserving the C_{2v} symmetry of the compound. As can be seen from the Schlegel diagram depicted in Figure 6, the C_2 axis dissects a carbon 6,6-bond and passes through the center of a six-membered ring. According to ref 6, the ion is slightly displaced from the center of gravity toward this six-membered ring. The local symmetry implies that hfi and nqi will also be

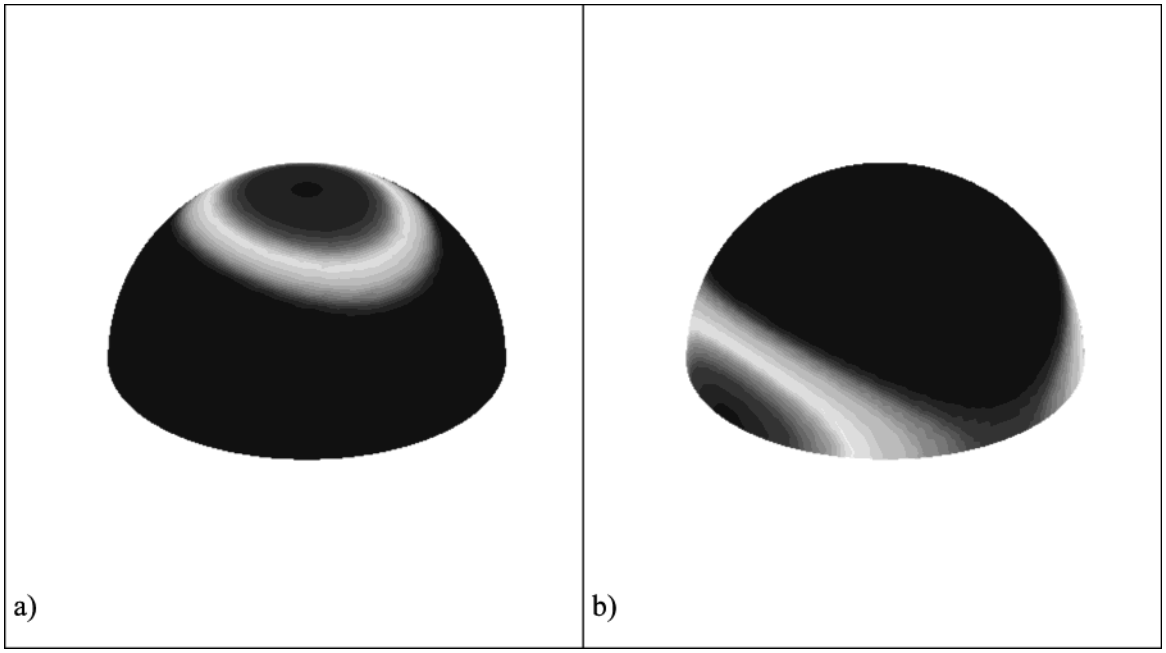

Figure 7. Calculated selection profile using *g*-matrix values given in the text. An excitation width of 20 MHz has been assumed for (a) $B \parallel z$ and (b) $B \parallel x$.

of nonaxial symmetry. The orientations of the principal axes of both tensors are expected to be collinear with those of the *g* matrix, however. As result, selection of canonical orientations is possible, if the spectral width of the microwave pulses is significantly less the dipolar hfi und if the field distribution induced by the *g*-matrix anisotropy is large enough. By use of the *g*-matrix values determined from a fit of the EPR spectrum, effective orientation selection could only be expected at the high field edge of the spectrum. In Figure 7, effective orientation selection is indicated for typical experimental conditions. Substantial "mixing" of perpendicular orientations cannot be avoided thus preventing the determination of y' and x' principal values of the dipolar and quadrupolar hfi. Instead, orientational averaging will lead to purely resolved ENDOR spectra, unless near axial prevails for both interactions.

In the case of La@C_{82}(I), spin-dephasing times of approximately 5 μs were observed, nearly independent of temperature. Spin−lattice relaxation rates were strongly temperature dependent and reached 5 ms at 10 K. Pulsed ENDOR spectra were recorded using a $\pi - T - \pi/2 - \tau - \pi$ Davies sequence ($\tau_{\pi/2} = 40$ ns, $T = 180$ μs, $\tau = 1$ μs), nuclear spin transitions being excited during interval T after the inverting π pulse. An effective $\pi/2$ pulse length of 40 ns was obtained using a multistage microwave amplifier,[12] boosting the 5 mW output of the commercial 94 GHz microwave bridge to 100 mW. Attempts to observe ENDOR signals with the standard low-power version ($\tau_{\pi/2} = 160$ ns) were not successful in this case. Even with this improved setup, ENDOR signals were extremely weak and were only detected after more than 10 h accumulation time. The resulting spectrum is depicted in Figure 8, combining the data files of several consecutive experiments, partially spanning overlapping frequency ranges.

In agreement with eq 1, equidistant transitions are observed, centered about the nuclear Zeeman frequency $\nu_n(^{139}\mathrm{La}) = 20.4$ MHz, the low-frequency multiplet, however, being barely detectable. Clear identification of transitions of the high-frequency multiplet nevertheless allows the unambiguous determination of all relevant parameters, viz., $|A_{z'z'}| = 5.9(2)$ MHz and $|Q_{z'z'}| = 0.44(2)$ MHz. As is indicated by the simulation,

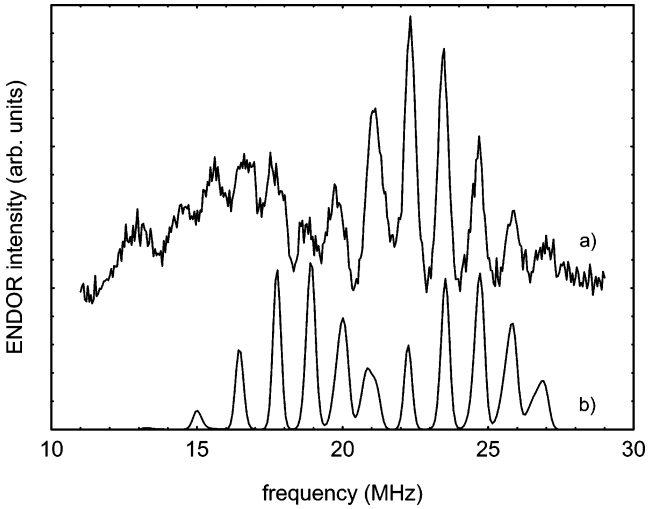

Figure 8. (a) W-band pulsed ENDOR spectrum of La@C_{82}(I) measured at 10 K at $B_0 = 3371.6$ mT. The spectrum was accumulated when exciting the high-field edge of the EPR spectrum and by invoking a Davies pulse sequence. (b) A simulated spectrum used to identify the individual line positions is also shown. For details, see text.

the expected seven-line pattern of both m_s multiplets, separated by $A_{z'z'}$, overlap partially.

To verify the assignment of the high-frequency part, spectra were taken using a sequence of slightly different field positions. The resulting ENDOR spectra are displayed in Figure 9. By use of the *g*-matrix given above and an estimated dipolar coupling tensor in combination with a microwave excitation width of 20 MHz, the change in the orientational selection profile can be calculated and is depicted in Figure 10. The excitation field values were chosen as 3371.6 mT (a) and 3369.2 mT (b), corresponding to the extreme values in Figure 9.

In Figure 9, the trivial shift of ENDOR frequencies resulting from a change of nuclear Zeeman frequency is removed by referencing each spectrum to the actual nuclear Zeeman frequency. As can be seen, the remaining effect of relaxed orientation selection results in a monotonic reduction of line distances and also in a change of line widths of individual

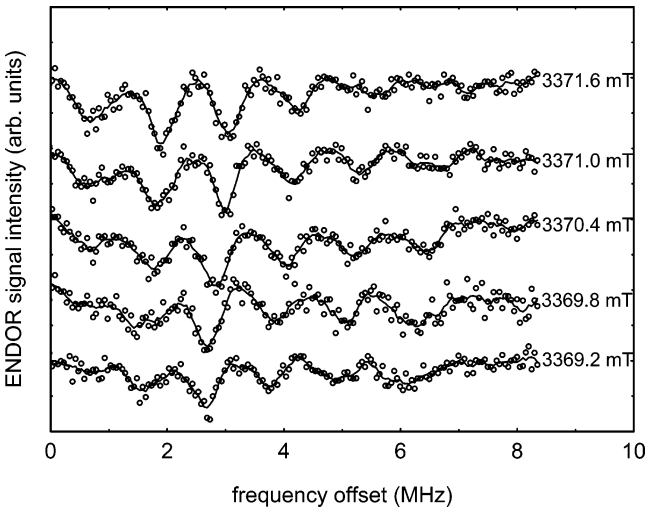

Figure 9. High-frequency ENDOR multiplet as function of microwave excitation. Incipient line broadening is observed when relaxing the orientation selection condition. In addition, the outermost ENDOR line, exhibiting a frequency offset of approximately 6.5 MHz, is only observed when exciting spin packets noticeably shifted from the outermost EPR transition. For details, see text.

components. Furthermore, the highest frequency line becomes more pronounced at smaller external field values used for microwave excitation. The observation that the predicted complete ENDOR line multiplet is not observed under all external field settings is not surprising because semiselective microwave pulses cannot cover the complete hyperfine EPR multiplet.

From Figure 9, we conclude that either $m_I = {}^7/_2$ and $m_I' = {}^5/_2$ or $m_I = -{}^7/_2$ and $m_I' = -{}^5/_2$; ENDOR transitions are not excited if microwave excitation is performed at the high-field edge (3371.6 mT) of the EPR spectrum. We can discriminate between both possibilities making the following assumptions. The eight-line EPR multiplet originating from molecules that are oriented parallel to z' ($\Theta = \Phi = 0$) spans a field range of $7 \times 5.9/28 = 1.475$ mT. If the sign of $A_{z'z'}$ is taken as positive like the sign of the isotropic hfcc, high-field edge EPR transitions can be assigned as connecting $m_I = -{}^7/_2$ nuclear spin levels. By use of this assignment, the high-frequency ENDOR multiplet can be labeled with $m_S = -{}^1/_2$. Vanishing of the highest-frequency ENDOR transition using high-field edge excitation implies that $Q_{z'z'} < 0$. (Taking $A_{z'z'}$ as negative instead, a positive sign of $Q_{z'z'}$ is predicted.)

The interpretation of the low-frequency part of the spectrum is less clear. Although part of the observed structure coincides with predicted line positions, additional peaks are not explained and are tentatively attributed to strong baseline variations.

In Figure 11, part of the weak ENDOR spectrum is shown, which is obtained when exciting with microwave pulses at the low-field edge (3357 mT) of the EPR spectrum. We tentatively assign the 4-line structure to the high-frequency part of the ENDOR multiplet, the prominent feature at 1.6 MHz being its center. Under this assumption, the effective hyperfine coupling constant amounts to 3.2 MHz. This value can be taken as average of $A_{x'x'}$ and $A_{y'y'}$, with unknown weighting coefficients. Apparently the deviation from axial symmetry is sufficiently large that line broadening because of orientational mixing becomes dominant. No further axis assignment is possible, because strong mixing of x' and y' components occurs under our experimental conditions. Attempts to improve orientation selection by using microwave pulses of reduced spectral width failed because of a decrease in signal-to-noise. It should be noted that the spectrum presented in Figure 11 was already accumulated for more than 10 h. Within this approximation, an estimate for the isotropic part of the hfcc is obtained as $({}^1/_3)\mathrm{tr}(A_{i'i'}) = 4.1$ MHz.

By use of the same approach to derive information about the quadrupole interaction, we note that the average value of $Q_{x'x'}$ and $Q_{y'y'}$ amounts to 0.63 MHz, larger than the value measured for the z' component. Because $Q_{i'i'}$ must be traceless, we have to conclude that $Q_{x'x'}$ cannot be the principal component of a nearly axial tensor in contrast to the dipolar interaction. This, however, is not at variance with symmetry constraints. All data

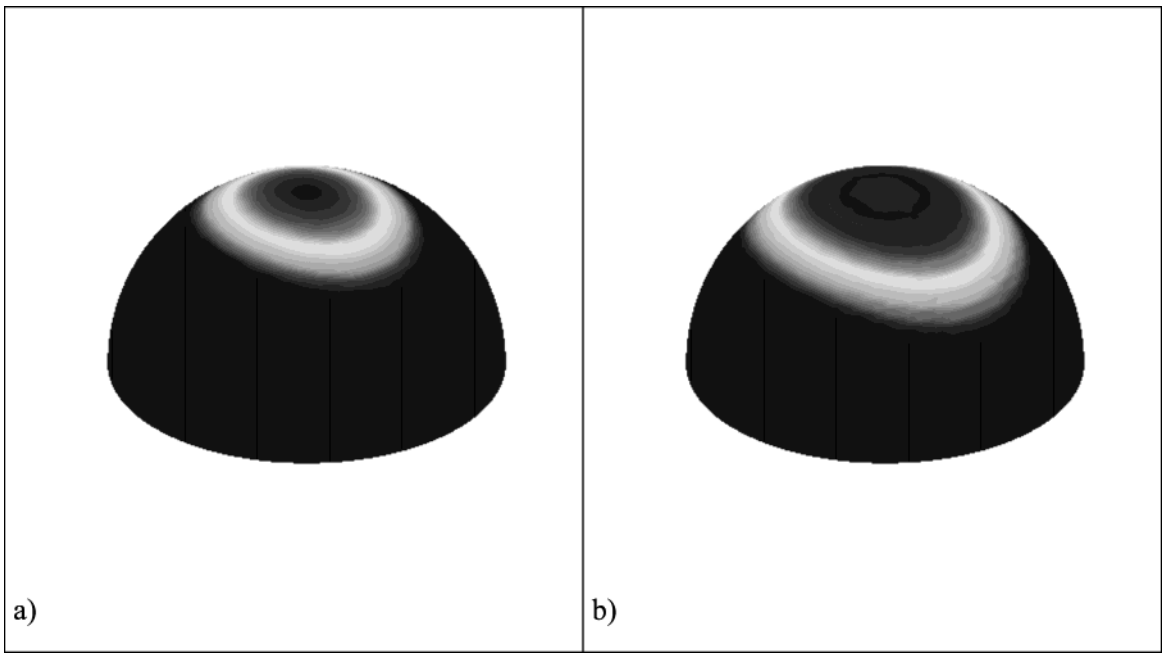

Figure 10. Calculated selection profile using *g*-matrix and hfi values given in the text. An excitation width of 20 MHz has been assumed. The excitation field values were chosen as 3371.6 mT (a) and 3369.2 mT (b), corresponding to the extreme values of the interval covered by selective excitation (see Figure 9).

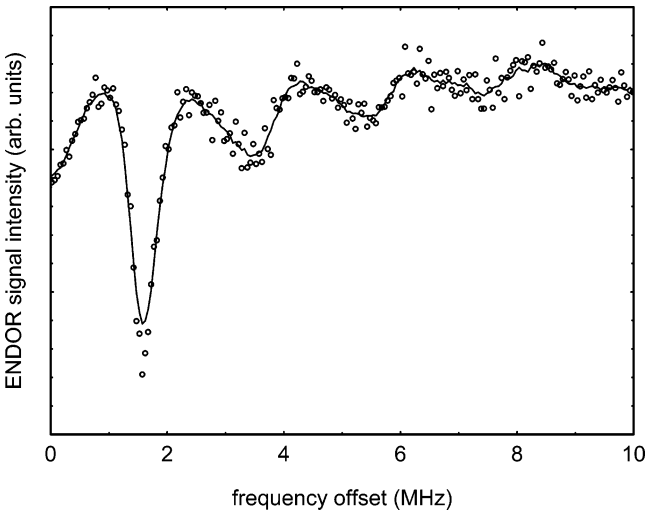

Figure 11. W-band pulsed ENDOR spectrum of La@C_{82}(I) measured at 10 K. The spectrum was accumulated when exciting the low-field edge of the EPR spectrum and using a Davies pulse sequence. The solid line is obtained by a sliding average of 7 data points.

TABLE 1: Compilation of Hyperfine Data

	La@C_{82} in solid solution (10 K)	La@C_{82} in liquid solution (200−300 K)
$\lvert A_{z'z'}\rvert$ (MHz)	5.9(2)	6.48;[a] 6.5(10)[b]
$\lvert(A_{x'x'}, A_{y'y'})\rvert$ (MHz)	3.2	1.6
a_{iso} (MHz)	4.1	3.36(1)−3.15(1)[c]
$\lvert Q_{z'z'}\rvert$ (MHz)	0.44(2)	
$\lvert(Q_{x'x'}, Q_{y'y'})\rvert$ (MHz)	0.63	
$e^2qQ/2I(2I-1)h$ (MHz)		0.85;[a] 0.85(2)[b]

[a] Reference 13. [b] Reference 4. For an estimate of the anisotropic hyperfine tensor components in solution, see text. [c] Schweitzer, P., Ph.D. Thesis, TU Darmstadt, 1997

derived from the analysis of ENDOR spectra are compiled in Table 1.

These values can be related to data determined from an analysis of the relaxation behavior of solution EPR spectra of La@C_{82}(I). Here, a consistent picture had emerged when fitting the widths of individual hyperfine components in the liquid-phase temperature range of 200−300 K. Values determined by two research groups are also compiled in Table 1. The value quoted for $A_{z'z'} = 6.5$ MHz is calculated from the observed dipolar anisotropy given as $\Delta A = |A_{\parallel} - A_{\perp}| = 4.89$ MHz and using $a_{iso} = 3.22$ MHz, which can be directly deduced from the resolved EPR spectrum. The principal axis of a pseudoaxial hyperfine tensor is defined as z'. A predicted average value for $A_{x'x'}$ and $A_{y'y'}$ of 1.6 MHz results using the "axial" approximation. It should be mentioned, however, that evaluation of relaxation data cannot give an axis assignment nor is it possible to accurately determine a deviation from axial symmetry. Although g-matrix and hfi tensor axes must be collinear, assigning the extreme g-matrix and hfi values to the same axis z' must be considered tentative.

Within this model, the dipolar hfi is nearly invariant over the full temperature range. The apparent lack of coincidence of the principal axis of dipolar and quadrupolar interactions precludes a direct comparison of $e^2qQ/2I(2I-1)h$ (solution, high temperature) with $|Q_{z'z'}|$ (solid, low temperature), the data indicating, however, a change of no more than a factor 2.

Conclusion

The analysis of EPR and ENDOR data obtained at different electron Larmor frequencies and in different phases leads to the conclusion that even at low temperatures no significant change occurs at the binding site of the encased ion. The structure of the binding site can be probed advantageously by using the lanthanum nuclear magnetic and electric quadrupole moments as sensors for the local spin and charge distribution. Apparently, the large-scale motion of the encased ion observed at room-temperature freezes, and because of averaging of hfis on the time scale of the EPR experiment, no drastic change of dipolar and quadrupolar hfi is observed. It should be noted, however, that the well-documented monotonous decrease of the isotropic La hfcc with temperature in the "high-temperature" solution phase[14] is consistent with the observed larger value at helium temperatures. Because this effect was related to anharmonic metal-to-cage vibrations, this can be taken as further evidence of continuous freezing of the large scale La motion.

The detection of hfi in disordered samples was possible only by using orientation selection in the 94-GHz EPR spectrum, which is expanded with respect to the magnetic field by g anisotropy. Quadrupolar hfi could be directly measured for the first time in this endohedral complex. The ability to observe frequency-resolved transitions between nuclear spin levels is clear proof that a unique La binding site exists in La@C_{82}. Such well-defined topology is a prerequisite to perform quantum-chemical calculations. It is a challenge to reproduce these results of spin and charge density distribution at the Lanthanum ion by quantum-chemical modeling. This will be essential for a better understanding of the electronic structure of the complex enabling for instance reliable predictions of oxidation and reduction potentials, which are important to understand the chemical reactivity of the compound.

Acknowledgment. Financial support by the Deutsche Forschungsgemeinschaft under various grants is gratefully acknowledged. German/Japanese collaboration was supported by a visiting professor fellowship and travel grants of the Institute for Molecular Science, Okazaki. We thank Dr. S. Stoll (ETH Zürich) for providing the EasySpin software package.

References and Notes

(1) Chai, Y.; Guo, T.; Lin, C.; Haufler, R. E.; Chibante, L. P. F.; Fure, J.; Wang, L.; Alford, J. M.; Smalley, R. E. *J. Phys. Chem.* **1991**, *95*, 7564.

(2) Johnson, R. D.; de Vries, M. S.; Salem, J. R.; Bethune, D. S.; Yannoni, C. S. *Nature* **1992,** *355*, 239.

(3) For a recent review, see: *Endofullerenes, A New Family of Carbon Clusters*; Akasaka, T., Nagase, S., Eds.; Kluwer Academic Publishers: Dordrecht, 2002.

(4) Ruebsam, M.; Schweitzer, P.; Dinse, K.-P. *J. Phys. Chem.* **1996,** *100*, 19310.

(5) Nishibori, E.; Takata, M.; Sakata, M.; Tanaka, H.; Hasegawa, M.; Shinohara, H. *Chem. Phys. Lett.* **2000,** *330*, 497.

(6) Takata, M.; Nishibori, E.; Sakata, M. In *Endofullerenes, A New Family of Carbon Clusters*; Akasaka, T., Nagase, S., Eds.; Kluwer Academic Publishers: Dordrecht, 2002.

(7) Andreoni, W.; Curioni, A. *Phys. Rev. Lett.* **1996,** *77*, 9606.

(8) Andreoni, W.; Curioni, A. *Appl. Phys.* **1998,** *A66*, 299.

(9) Okubo, S.; Kato, T.; Inakuma, M.; Shinohara, H. *New Diamond Front. Carbon Technol.* **2001**, *11*, 285.

(10) Weiden, N.; Goedde, B.; Käβ, H.; Dinse, K.-P.; Rohrer, M. *Phys. Rev. Lett.* **2000,** *85*, 1544.

(11) Knorr, S.; Grupp, A.; Mehring, M.; Kirbach, U.; Bartl, A.; Dunsch, L. *Appl. Phys.* **1998,** *A66*, 257.

(12) The add-on unit was produced by W. Krymov.

(13) Okubo, S. and Kato, T. *Appl. Magn. Reson.* **2003,** *23*, 481.

(14) Solodovniko, S. P.; Tumanskii, B. L.; Bashilov, V. V.; Sokolov, V. I.; Lebedkin, S.; Krätschmer, W. *Fullerene Sci. Technol.* **2000**, *8*, 1.